Automated phenotyping of mosquito larvae enables high-throughput screening for novel larvicides and offers potential for smartphone-based detection of larval insecticide resistance

Steven D. Buckingham[1†], Frederick A. Partridge[1†], Beth C. Poulton[1,2†], Ben Miller[3†], Rachel A. McKendry[3,4] Gareth J Lycett[2] and David B. Sattelle[1*]

[1]UCL Centre for Respiratory Biology, UCL Respiratory, Division of Medicine, Rayne Building, 5 University Street, London WC1E 6JF, UK.

[2]Liverpool School of Tropical Medicine, Pembroke Place, Liverpool, Merseyside, L3 5QA, UK.

[3]London Centre for Nanotechnology, Faculty of Maths & Physical Sciences, University College London, 17-19, Gordon Street London, WC1H 0AH, UK.

[4]Division of Medicine, UCL, Rayne Building, 5 University Street, London WC1E 6JF, UK

†These authors contributed equally; * To whom correspondence should be directed

Abstract

Pyrethroid-impregnated nets have contributed significantly to halving the burden of malaria but resistance threatens their future efficacy and the pipeline of new insecticides is short. Here we report that an invertebrate automated phenotyping platform (INVAPP), combined with the algorithm Paragon, provides a robust system for measuring larval motility in *Anopheles gambiae (and An. coluzzi)* as well as *Aedes aegypti* with the capacity for high-throughput screening for new larvicides. By this means, we reliably quantified both time- and concentration-dependent actions of chemical insecticides faster than using the WHO standard larval assay. We illustrate the effectiveness of the system using an established larvicide (temephos) and demonstrate its capacity for library-scale chemical screening using the Medicines for Malaria Venture (MMV) Pathogen Box library. As a proof-of-principle, this library screen identified a compound, subsequently confirmed to be tolfenpyrad, as an effective larvicide. We have also used the INVAPP / Paragon system to compare responses in larvae derived from WHO classified deltamethrin resistant and sensitive mosquitoes. We show how this approach to monitoring larval response to insecticides can be adapted for use with a smartphone camera application and therefore has potential for further development as a simple portable field-assay with associated real-time, geo-located information to identify hotspots.

Author summary

We have developed an automated platform for recording the motility of mosquito larvae and applied it to larvae of a mosquito vector of malaria and a mosquito vector of dengue, Zika, yellow fever and other human diseases. The platform facilitates high-throughput, chemical screening for new compounds to control mosquito larvae and also detects differences in response in larval progeny from pryethroid resistant adult mosquitoes. Pyrethroid-impregnated bednets have helped to halve the deaths from malaria in recent years but pyrethroid resistance is an important threat to this progress. Our approach assays insecticide actions faster than the current WHO standard test and we show that it can be adapted for use with a smartphone, which offers the prospect of a future field assay to monitor developing resistance associated with behavioural response with the added benefit of precise satellite-based location.

Introduction

Mosquito-borne pathogens kill more than one million people every year, while severely debilitating diseases including malaria, dengue, Zika, West Nile virus, chikungunya, yellow fever and Japanese encephalitis, transmitted by these vectors cause suffering for hundreds of millions. Successful attempts to control the incidence of such diseases have mainly targeted mosquito population size and hence infective biting frequency [1]. As a result, the burden of malaria has been halved in the period 2000-2015, mostly due to the use of insecticide-treated nets (ITNs) containing pyrethroids, which target the adult disease-transmitting Anopheles mosquitoes that tend to feed nocturnally in homes [2]. However, the future efficacy of ITNs to control malaria is threatened by growing mosquito resistance to the available pool of insecticides [3] and by an increase in the prevalence of Anopheles mosquitoes that blood-feed outdoors [4].

ITNs are of limited use against viral pathogens transmitted by *Aedes aegypti* mosquitoes, such as dengue, Zika, yellow fever and chikungunya, since the adult vectors favour feeding at dawn and dusk. The ineffectiveness of ITNs against Aedes and the absence of drugs or vaccines for most vector-borne viruses means that a mainstay of viral disease control has been larval source management (LSM) [5]. This integrated approach targets aquatic egg-laying sites with the aim of reducing the number of immature forms, leading in turn to fewer biting adults. LSM can incorporate community environmental measures to limit temporary aquatic breeding sites in and around homes, as well as the application of larvicidal agents, such as temephos, to important, permanent water sources. These traditional LSM methods are effective where the breeding sites that produce the majority of adults can be readily identified and treated accordingly [6]. Alternative methods, attempting to overcome this limitation, involve the dusting of resting female mosquitoes with highly potent larval growth inhibitors. As a result, growth inhibitors are delivered to oviposition sites at doses proportional to the frequency of visits. By this means, the most important breeding sites are targeted [7].

For malaria control, there is growing awareness that LSM may have a more prominent role to play under certain situations, complementing adult-targeted insecticide interventions. Examples include: targeting zones where the prominent vectors rest and feed outdoors; tackling transmission foci, where saturating ITN usage is having limited effect on disease transmission; deployment in areas where adults are resistant to all known insecticides; treatment of urban areas in which water sources that suit Anopheline development may be more readily identified [8]. Technologies, such as drones and mapping have been combined to improve identification and prioritisation of habitats in rural areas

[9,10]. There may be additional opportunities to control multiple larval mosquito species simultaneously that will affect both malaria and viral disease transmission [6].

Larvicides in current use include surface oils and films that suffocate immature forms, bacteria (including *Bacillus thuringiensis* that produces toxic protein crystals that target the larval midgut), insect growth regulators (including pyriproxyfen that inhibits adult emergence) and synthetic chemicals (such as chlorpyrifos, pirimiphos-methyl and temephos) that target the insect nervous system [6] .

Standardized methods to examine relative larval susceptibility to compounds are necessary to maintain the effective deployment of current larvicides by identifying the emergence of resistance in mosquito populations [11]. Moreover, a high-throughput method to screen larvicides would offer the possibility to examine large chemical libraries for new classes of compounds. Currently the World Health Organisation issues guidelines for larvicidal toxicity assays [12], which consist of exposing larvae in small cups to increasing doses of chemical and manual observation of mosquito killing. In such assays, larval death is defined by the moribund appearance of larvae and their failure to respond to tapping of the cup. This is labour-intensive and the end-point can be difficult to assign unambiguously.

We have developed an automated phenotyping assay based on larval motility, which is simple to deploy, provides a fast readout and, being multi-well plate based, offers much needed high-throughput screening capabilities. Our system uses an INVertebrate Automated Phenotyping Platform (INVAPP) previously described for monitoring nematode motility in conjunction with the Paragon

algorithm to estimate motility from moving images of larvae [13]. We illustrate the capability of our system by (a) quantifying the actions of the larvicide temephos on larval motility, (b) screening a chemical library, which showed larvicidal actions of tolfenpyrad and (c) detecting differential responses in larval progeny from deltamethrin resistant and susceptible *Anopheles coluzzii* and *Aedes aegypti* mosquitos. We also demonstrate the potential for its further development as a smartphone-based field assay, for rapid detection of behavioural change related to pyrethroid resistance, using the inbuilt camera to track larval motility.

Methods

Mosquito rearing and strains

The mosquito strains used are established colonies which have been characterised by WHO protocols as either deltamethrin sensitive or resistant in female adults. They have been in lab culture for 2 - 20 years and were not infected with any known pathogen. Resistant (Cayman) and sensitive (New Orleans) *Ae. aegypti* strains and resistant *An. coluzzii* (Tiassale) and sensitive *An. gambiae* (G3) strains were studied. The resistant lines were obtained from LITE (https://lite.lstmed.ac.uk/lite-facilities/lite-insectaries), which regularly (approx. every 3 months) select adults with permethrin/deltamethrin. Cayman show between 20-50 % mortality and Tiassale 10-20% moratality to deltamethrin in standard WHO bioassays. These strains are not characterised routinely for larval resistance to temephos and deltamethrin. Previous assays on the Cayman larvae indicated a 1.64 resistance ratio compared to the New Orleans strain (Harris 2010). The mosquito batches maintained at LSTM and provided to UCL were not further selected prior to despatch. It should be noted that there exists a considerable degree of genetic variation in Anopheline mosquitoes especially in the species complex *Anopheles gambiae sensu lato*, which is widespread in sub-Saharan Africa. *Anopheles gambiae* and *Anopheles coluzzii* are morphologically indistinguishable species and were for many years considered as distinct molecular forms (S and M respectively) of the same species. The G3 strain we here deploy has always been called *Anopheles gambiae* but is in fact a hybrid of molecular forms. Pure *An. coluzzii* strains can be found in Tiassale, Cote D'Ivore, but the lab strain Tiasalle 13 deployed here is also a hybrid.

129 ***Larval hatching and maintenance***

130 ***Anopheles***

131 Anopheles eggs laid day 1 evening or day 2 morning were shipped securely from Liverpool School of
132 Tropical Medicine (LSTM) to University College London (UCL) on filter paper ensuring that they remain
133 moist throughout the journey. At UCL on day 3, eggs were washed into a shallow dish containing
134 deoxygenated (pre-boiled and cooled) water containing 0.001% pond guardian tonic salt (Blagdon) to
135 a depth of about 2.5 cm. The eggs and newly-hatched larvae were maintained at 25°C. Larvae were
136 fed 1/3 pellet of cat food per dish and tested on days 5-6.

137 ***Aedes aegypti***

138 *Ae. aegypti* egg papers were shipped securely to UCL from LSTM and stored at room temperature for
139 up to 1 month. They were hatched over 1-2 days by placing the egg papers in a tray of deoxygenated
140 (pre-boiled and cooled) tap water to which a crushed yeast tablet (Holland and Barrett) had been
141 added. Larvae were tested on days 3-4.

142 ***Harvesting larvae and transfer to 96-well plates***

143 Experiments were performed on larvae 1-2 days post hatching and thus a mix of first and early 2nd
144 instar larvae. The water in which larvae were swimming was passed through a 100 µm Nylon mesh
145 cell-strainer (Fisher Scientific) to concentrate the larvae. This concentrated suspension of larvae was
146 diluted until 100 µL of suspension contained 5-10 larvae. A 100 µL aliquot of this suspension was
147 added using a standard Gilson pipette to each well of a 96-well plate, with the tip of the pipette being
148 cut back to reduce damage to the larvae. Subsequently, 100 µL of the compound under test was

added (dissolved in water from a 10^{-2}M DMSO stock to yield the required final concentration of 10^{-4}M). Wells containing DMSO alone diluted to appropriate concentrations served as controls.

Filming larvae using INVAPP and analysis of motility using Paragon

Larvae were filmed using INVAPP, a device for monitoring invertebrate motility that is well suited to high-throughput chemical screening and has been deployed for the study of nematode motility (11). INVAPP consists of an Andor Neo "sCMOS" camera (2560 x 2160 resolution, maximum 100 frames per second frame rate) fitted with a Pentax YF3528 line-scan lens. The camera is mounted beneath a microplate supporting platform illuminated from above by an LED array panel. An acrylic diffuser ensures that the field of view of the camera is evenly lit (Figure 1).

Images (total = 30) were acquired every 10 ms. This was repeated at approximately 5 s intervals until 5 or 10 series of image sequences were obtained. Acquiring images at this rate detected the slow, drifting movements associated with filter feeding as well as rapid "jumping" that larvae undergo at sporadic intervals. For every plate, in addition to filming at selected time points, readings were collected immediately prior to addition of chemicals. Image sequences were stored offline for later analysis. This was performed at least three times in separate weeks with each of the three replicates consitituting one data point in the analysis (i.e. at least three biological replicates).

Paragon algorithm

The analysis uses an implementation of the Paragon algorithm [13, https://github.com/fpartridge/invapp-paragon] and is described in outline below:

1. Read frames 1, 11 and 21 of the image sequence into a $n \times m \times 3$ array where n, m are the height (approximately 700 pixels) and width (approximately 950 pixels) of the image sequences.

2. Calculate the variance in the time dimension

3. Identify the pixels for which the variance exceeds the mean by 3 standard deviations:

$$\left\{\begin{matrix} 1 if x_i > mean(x) + 3 \times std(x); \\ 0 if x_i \leq mean(x) + 3 \times std(x) \end{matrix}\right\}$$

4. For each well, count the number of pixels of value 1 to produce a *Movement Index*

5. Normalize the movement index for all time points by dividing it by the value obtained for movies acquired immediately before adding compounds.

The procedure was performed three times and the median value is taken as the output of the screen. Image processing and inferencing was performed with Python scripts utilizing the following publicly available software libraries: Numpy, Pandas, Scikit-Image and Statsmodels. Matplotlib and Seaborn software libraries were employed for plotting.

Filming a plate requires 5 (in some cases 10) image sequences to be made each with 30 frames at 10 ms intervals, requiring a total of about 1 s for each image sequence. Analyzing one movie takes approximately 3 s on a desktop computer. The speed of recording and analysis permits library-scale screening of re-profiled and novel, candidate insecticide chemistry.

Estimation of pIC50

The pIC50 were estimated by fitting the concentration and the movement index to the expression:

$$M = \frac{1}{1 + 10^{\frac{I-C}{H}}}$$

Where M is the predicted normalized movement index (the index measured after the application of compound divided by that measured before), I is the IC50, C is the concentration of the compound and H is the slope. Fitting was done by the least squares method using the Python "Scipy" package. The pIC50 is the -log10 of the IC50.

Chemicals

Temephos, an organophosphate anti-cholinesterase and established mosquito larvicide, was obtained from Sigma Aldrich (Item 31526-250MG). Deltamethrin (DM) is a pyrethroid insecticide used in bednets for which acts on insect sodium channels [14–16] and was obtained from Chem Service (Item N-11579). This particular pyrethroid was selected for study as the strains used had previously been characterised for deltamethrin resistance in the adult stage, and we were keen to examine if resistance could also be detected during larval stages using the INVAPP / Paragon system. Temephos and deltamethrin were prepared as stock solutions (1×10^{-2} M in DMSO) then diluted to the required final concentrations in water.

The Medicines for Malaria Venture Pathogen box library contains 400 drug-like molecules targeting a wide range of neglected tropical diseases. We used this to explore the potential of library-scale drug screening using INVAPP / Paragon.

Smartphone-based detection of motility

The smartphone application software was written using Android Studio with the OpenCV 3.3.0 library to implement a camera, handling the RAW pixel values in real time. The smartphone used was an LG G4 (16 MP, f/1.8, 28mm). After adding the larvae to wells of a 96 well plate and leaving to settle, recording is initiated with the phone camera pointing at the well plate. The application then automatically initialises two 1D arrays for the real-time mean and variances of each pixel. On each

camera frame, the raw pixel values are extracted as a 1D byte array and converted to a float array. The mean and variance matrices are updated with the following formulae:

$$M_n = M_{n-1} + \frac{P - M_{n-1}}{n}$$

where, M is the mean matrix, P is the pixel value matrix and n is the number of frames.

$$V_n = \frac{(n-1)V_n + (P - M_{n-1})(P - M_n)}{n}$$

where V is the variance matrix.

After 60 frames, the mean and variance matrices are exported as a text file. This measurement is repeated every 10 s. The frame-rate, and therefore sensitivity, depends on the resolution of the image. Here, 320×240 images are used, giving around 30 frames per s, and therefore 2 s measurements every 10 s.

The variance matrix gives high values for areas of the frame where there is high motility (i.e in the wells with high larval motility), and low values (noise) between wells. This matrix can then be segmented into regions of interest (wells with larvae). This is a flexible approach, allowing measurement of a whole plate, or parts of a plate, depending on the framing.

At t=200 s, deltamethrin or control (water) was added to each well, and the variance tracked over time as described. After segmenting the regions of in interest, the variance at each time point for each well is calculated by taking the mean of the variance in the well. These are then plotted over time, showing the variance change with time. The resulting time-variance plots are fitted to exponential a decay function (Mathematica 11.3):

$$V_t = A + B\exp^{-k(t-T)}$$

224 where V is the variance, A is the baseline variance, B is the maximum variance due to the larvae, k is
225 the variance decay rate, and T is the time when the variance begins to decrease.

226 The fitted values for k are used to distinguish between susceptible and resistant larvae.

227 ***WHO Larval Assay***

228 The WHO larval assay was published in 2005 with the aim of standardizing testing of compounds for
229 their larvicidal actions on mosquitoes. It provides a detailed protocol for quantifying these toxic
230 actions of insecticides on mosquito larvae in the field and in the laboratory and is available from
231 https://apps.who.int/iris/bitstream/handle/10665/69101/WHO_CDS_WHOPES_GCDPP_2005.13.pdf.
232 Briefly, a quarter yeast tablet (Holland and Barrett) was added to 200 ml of dH_2O containing 0.001%
233 pond salt (Blagdon), prior to addition of 25 third-instar *Ae. aegypti* (New Orleans or Cayman) larvae
234 per cup. The appropriate volume of deltamethrin stock (dissolved in acetone) was then added to
235 achieve the desired concentrations (5×10^{-10} – 1×10^{-6} M respectively). The assays were performed in
236 triplicate and repeated three times on different larval batches. Mortality was assessed visually after 24
237 h continuous exposure.

238

239 **Results**

240 ***Using the INVAPP system to study the actions of the larvicide temephos on larvae of* Aedes aegypti**

241 Mosquito larvae swim [17,18] , jump [19] and rest [18]. Filming at 1 frame every 10 miliseconds
242 ensures that all types of larval movements are captured, but in accordance with the system's goal of
243 producing a rapid and simple index of larval activity these activities are not distinguished – the system
244 simply "decides" how much area in the image has seen movement of any kind. Temephos, a widely
245 used larvicide targeting *Ae. aegypti,* was tested on susceptible larvae of this species. A concentration-
246 dependent reduction in motility was detected after 240 min exposure to this larvicide (Fig. 1, bottom
247 right panel). Thus, the INVAPP / Paragon system enables robust, automated detection of larval motility
248 and the severe motility impairment resulting from exposure to the larvicide temephos.

249 ***Screening a chemical library for compounds with larvicidal activity***

250 Given the system's ability to provide a monitor of impaired motility in the presence of an established
251 larvicide, we tested the system using a small chemical library, the Medicines for Malaria Venture
252 (MMV) Pathogen Box. This library was supplied as 1.0×10^{-2} M solutions in DMSO and was further
253 diluted in DMSO to generate a 1.0×10^{-3} M stock of each compound. The library was then screened
254 against *An. gambiae* using the INVAPP / Paragon system; all chemicals from the collection were
255 initially tested at 1.0×10^{-5} M, n = 3, 1% v/v final DMSO. The actions of each chemical on the
256 movement index was recorded and ranked by their median (see supplementary data Table S1), and
257 the 5 compounds that most reduced the motility index (MMV007803, MMV637229, MMV687775,
258 MMV687776, MMV688934) were used in further analysis. All 5 were re-sourced in powder form as a
259 kind gift of MMV, prepared as a fresh DMSO stock, and tested for concentration-dependent actions
260 over the range 3×10^{-7} - 1×10^{-4} M for both the G3 and Tiassale 13. Of these compounds, MMV688934

261 (tolfenpyrad) showed a marked concentration-dependent immobilization of larvae (Fig. 2).
262 Tolfenpyrad is an inhibitor of complex I of the respiratory electron transport chain in the mitochondria.
263 It has been successfully trialled in toxic sugar baits to kill mosquitoes [20]. A weaker action was
264 observed for MMV637229 (Clemastine, a first-generation antihistamine for the treatment of hayfever)
265 which has also shown to be effective in killing *Trypanosoma cruzi* and *Plasmodium falciparum* [21,22].

266 ***Detecting motility differences in larval progeny from resistant and sensitive An. coluzzii and Ae.***
267 ***aegypti***

268 We tested whether our INVAPP / Paragon system was able to detect behavioural differences in larvae
269 derived from resistant compared to susceptible strains. Larvae from deltamethrin susceptible and
270 resistance strains were examined for each species (G3 [susceptible] and Tiassale 13 [resistant] for
271 Anopheles, and New Orleans [susceptible] and Cayman [resistant] for *Ae. aegypti*). Image sequences
272 were filmed immediately before addition of Deltamethrin and at intervals (2, 5, 10, 20, 45 and 60 min)
273 afterwards.

274 There was a concentration-dependent action of deltamethrin on motility for the 4 different strains
275 (Fig. 3). The concentration dependence was detected after 5 min of exposure. At briefer exposures
276 larvae were not completely immobilized, whereas at exposures longer than 60 min even the lowest
277 concentrations tested had immobilized all larvae. The curves for the 4 strains after 60 min exposure to
278 deltamethrin were fitted to a sigmoid function (see Methods), from which PIC_{50}s were estimated.

279 The PIC_{50} for Tiassale was estimated to be 7.0 ± 1.0 (100 nM), while that for G3 was estimated to be
280 8.0 ± 1.0 (10 nM). Similarly, the PIC_{50} for Cayman was estimated to be 8.0 ± 1.0 (10 nM), while that for
281 New Orleans was estimated to be 9.0 ± 0.0 (1 nM). The differences between susceptible and resistant
282 strains were statistically significant (2-way ANOVA, $F(1.0,24.0) = 7.0$, $P = 0.016$) but no significant

283 difference was detected between genus (2-way ANOVA, $F(1.0,24.0) = 3.0$, $P = 0.091$) and there was no
284 statistically significant interaction between genus and susceptibility (2-way ANOVA, $F(1.0,24.0) = 0.0$, P
285 $= 0.906$). Hence, the algorithm detected a more rapid decline in movement in larvae derived from
286 resistant adults after exposure to deltamethrin in both Anopheles and Aedes species.

287 ***Comparison of INVAPP / Paragon data with the standard WHO assay***

288 To determine how the Paragon algorithm compared to the WHO larval assay, we tested the *Ae.*
289 *aegypti* New Orleans and Cayman strains for deltamethrin resistance with traditional larval cup
290 bioassays (Fig. 4). The WHO assay yielded $\log LC_{50}$s of 8.60 ± 0.04 (LC50 = 2.5 nM) and 7.29 ± 0.14
291 (LC50 = 51.3 nM) for New Orleans and Cayman respectively (2-tailed, independent t-test, $T(4)=-3.9$,
292 $P=0.0$). The inhibition and resistance ratios estimated from the two methods by dividing the
293 respective LC50s. Hence, the resistance ratio estimated from WHO assays is similar to the inhibition
294 ratio obtained from Paragon. This suggests that the inhibition of movement at the 4hr time point in
295 the Paragon assay correlates well with the 24hr killing observed in WHO assays.

296 ***Smartphone detection of motility differences between pyrethroid susceptible and resistant strains***
297 Larvae were dispensed into a petri dish or 96 well plate and allowed to settle. Films of 2000-3000 s
298 duration were made at the smartphone camera default settings (LG G4: 16 MP, f/1.8, 28 mm). The
299 INVAPP/Paragon algorithm was then applied with no changes other than the threshold for allocating a
300 pixel as “having movement” or “not having movement”. In the absence of deltamethrin both larval
301 strains yielded a roughly constant movement index over the duration of the recording (Fig. 5A, B,
302 dotted lines). In the presence of 1×10^{-6} M deltamethrin, the movement index began to fall after
303 about 500-1000 s to a steady-state, low level. The rate of this decline was slower for larvae from
304 resistant strains ($\tau = 0.18 \pm 0.08 \times 10^{3}\ s^{-1}$ for Cayman and $3.5 \pm 0.16 \times 10^{3}\ s^{-1}$ for Tiassale) than it was

for larvae from susceptible strains ($\tau = 2.7 \pm 0.2 \times 10^3\ s^{-1}$ for New Orleans and $12 \pm 2.3 \times 10^3\ s^{-1}$ for G3 – *Anopheles:* one-tailed unpaired t-test $T(4) = 7.0$, $P = 0.003$; *Ae. aegypti:* one-tailed unpaired t-test $T(4) = 20.0$, $P < 0.001$). Thus, INVAPP/Paragon detected the differential response of the larval progeny from resistant strains for two significant human disease vectors following short term exposure to 1 µM deltamethrin in real-time on a readily available smartphone.

Discussion

Here we evaluate the utility of an automated screening platform / algorithm combination in quantifying the actions of chemicals tested against mosquito larvae for their capacity to impair larval motility. Previously, the "INVertebrate Automated Phenotyping platform (INVAPP), with the Paragon algorithm [13] had been shown to enable high-throughput chemical screening on the nematode genetic model organism *C. elegans* and parasitic nematodes such as *Haemonchus contortus, Teladorsagia circumcincta,* and *Trichuris muris* worms in the search for novel anthelmintic candidates [13]. The system allows 96 well plate-based chemical screening for anthelmintic activity. By this means we detected compounds affecting the motility and development of worms. We deployed known anthelmintics to validate the utility of the INVAPP/Paragon system and screened the MMV Pathogen Box chemical library identifying compounds already known to have anthelmintic or anti-parasitic activity and other compounds previously not known to have anthelmintic activity [13,23]. In separate studies we showed how this approach could help identify novel classes of chemistry with anthelmintic activity, the dihydrobenz[e] [1,4] oxazepin-2 (3*H)*-ones [24,25] and the 2,4-diaminothienol [3,2-*d*] pyrimidines [26].

Here we demonstrate the use of INVAPP paired with the analysis algorithm Paragon as a rapid, convenient and robust method for estimating a biologically-relevant parameter (motility) of the behaviour of mosquito larvae from two key human disease vectors. It was first used to detect the actions on motility of *Ae. aegypti* larvae of a known larvicide, temephos. Following this validation of the ability of INVAPP / Paragon to detect larval motility impairment by an established larvicide, we

333 explored its potential use in library-scale chemical screening. The discovery of new and re-profiled
334 insecticidally-active chemicals remains important. As a proof-of- principle exercise, we screened
335 (blind) a 400-compound library – The Medicines for Malaria Venture (MMV) Pathogen Box. We
336 identified tolfenpyrad, an established insecticide, as a toxic agent for mosquito larvae. Tolfenpyrad is a
337 pyrazole insecticide developed by the Mitsubishi Chemical Corporation in 1991. It is active against
338 adults of the Anopheles strains used in this study (Lees et al 2020), whiteflies [27] and aphids [28] as
339 well as *H. contortus* [29] . Since tolfenpyrad is the only known insecticide in the MMV Pathogen Box,
340 this is indicative of the specificity of the screen.
341
342 As well as readily identifying the potent insecticide, tolfenpyrad, our screen of the MMV Pathogen Box
343 also showed that clemastine has a paralysing action on mosquito larvae, suggesting that the algorithm
344 can be useful in high throughput chemical re-profiling screens. Clemastine is a sedating anti-
345 histaminergic drug used in the treatment of allergic reactions, including seasonal allergic rhinitis ("hay-
346 fever") [30]. In vertebrates it blocks primarily the H1-subytpe of histamine receptor, which is a
347 member of the 7-transmembrane, G-protein-coupled receptor family [31]. Insects are known to use
348 histamine as a neurotransmitter and to possess a histamine-gated chloride channel with some
349 pharmacological similarities to the vertebrate H1 class [31,32]. Perhaps of equal interest is the fact
350 that histamine-gated chloride channels are not present in vertebrates [33] and insects do not possess
351 a metabotropic histamine receptor [34]. Cys-loop ligand-gated anion channels are known targets of
352 insecticides and anthelmintics [35,36]. It has also been reported that mutations in the two Drosophila
353 histamine-gated chloride channels (HClA and HClB) have opposite effects on ivermectin sensitivity:
354 mutation of HClA confers enhanced sensitivity whereas knockout of HClB diminished sensitivity to
355 avermectin neurotoxins [37,38], suggesting that these channels as well as GluCls may play a role in

356 the action of macrocylic lactone derivatives. Furthermore, the finding that two histamine-gated
357 chloride channels cloned from the housefly, *Musca domestica*, are insensitive to other insecticides
358 known to target GABA and glutamate-gated ion channels [39] suggests that histamine-gated chloride
359 channels may have a very distinct pharmacological profile offering a quite new candidate insecticidal
360 target. However, it should be noted that neither HClA [40] nor HClB [41] null mutants are lethal,
361 suggesting a possible limitation on the usefulness of these receptors as targets of insecticides.
362
363 Resistance to drugs and chemicals used to combat malaria seriously threatens the success of control
364 measures and the investment therein over the past 15 years. The widespread emergence of
365 pyrethroid resistance threatens the hitherto successful deployment of ITNs [3,41]. Resistance in the
366 adult mosquito vectors is established but much less is known concerning resistance in mosquito larvae
367 for which targeting by larvicides is a valid control approach especially for *Ae. aegypti*. Here using
368 behavioural phenotyping, we have shown that comparison of susceptible and resistant *Ae. aegypti*
369 larvae, produced a ratio of reduction in movement index that was similar to the resistance ratio
370 determined through WHO assays. A comparative reduction in motility was also observed following
371 exposure of Anopheles larvae from strains where the adults show WHO resistant phenotypes. These
372 findings are robust in our laboratory studies, but will require the analysis of more resistant strains to
373 determine the precise predictive nature of INVAPP / Paragon measurements compared to WHO
374 classified resistance ratio. In future, it will also be of interest to explore whether dual larvicidal
375 treatments can help combat resistance and whether the INVAPP / Paragon system can be used to
376 assist in identifying new areas of chemistry and / or new targets not already compromised by known
377 resistance mechanisms that will be needed for such approaches.
378

INVAPP combined with the Paragon algorithm would allow for faster measurement than can be accomplished using the currently deployed manual WHO assay for larvicidal activity. It may not be as sensitive as the manual assay, but it allows the effectiveness of compounds to be measured more rapidly, and provides more detail in the time-dependence of the actions of compounds to be identified. It also requires a smaller bench footprint and is less labour intensive. Also, manual assays such as the current WHO assay are subject to investigator fatigue and the end-point assessment is not always straightforward. INVAPP / Paragon, which is automated, reduces errors due to these factors.

Increasingly, sensitive smartphone applications and cameras are being used for the diagnosis and study of infectious diseases including malaria. For example, a smartphone polarised microscope has been used for malaria diagnosis [42]. Automated detection of malaria parasites in blood smears has been achieved [43,44]. A rapid and robust field detection of resistance that utilises a simple smartphone assay could also yield valuable information. Geo-located data on larval resistance could be readily transmitted to central databases that provide regional information of the temporal and spatial development of insecticide resistance which can be mapped alongside the emergence of adult resistance and malaria prevalence data [45,46]. We have shown potential to detect differences in behavioural response to a pyrethroid insecticide using a smartphone camera. This paves the way for the development of a smartphone application perhaps to be used in conjunction with a simple, slide-on test kit that will facilitate such measurements. These assays are a promising first step in developing such a simple-to-operate field assay.

Acknowledgements

We thank Medicines for Malaria Venture for the Pathogen Box library and resupply of hit compounds.

References

1. Curtis CF, Jana-Kara B, Maxwell CA. Insecticide treated nets: impact on vector populations and relevance of initial intensity of transmission and pyrethroid resistance. J Vector Borne Dis. 2003;40: 1–8.

2. Bhatt S, Weiss DJ, Mappin B, Dalrymple U, Cameron E, Bisanzio D, et al. Coverage and system efficiencies of insecticide-treated nets in Africa from 2000 to 2017. Kyobutungi C, editor. eLife. 2015;4: e09672. doi:10.7554/eLife.09672

3. Hemingway J, Ranson H, Magill A, Kolaczinski J, Fornadel C, Gimnig J, et al. Averting a malaria disaster: will insecticide resistance derail malaria control? The Lancet. 2016;387: 1785–1788. doi:10.1016/S0140-6736(15)00417-1

4. Russell TL, Beebe NW, Bugoro H, Apairamo A, Chow WK, Cooper RD, et al. Frequent blood feeding enables insecticide-treated nets to reduce transmission by mosquitoes that bite predominately outdoors. Malar J. 2016;15: 156. doi:10.1186/s12936-016-1195-8

5. Medical Entomology for Students. 5 edition. Cambridge: Cambridge University Press; 2012.

6. Larval source management: a supplementary measure for malaria vector control: an operational manual. Geneva: World Health Organization; 2013.

7. Devine GJ, Perea EZ, Killeen GF, Stancil JD, Clark SJ, Morrison AC. Using adult mosquitoes to transfer insecticides to *Aedes aegypti* larval habitats. Proc Natl Acad Sci. 2009;106: 11530–11534. doi:10.1073/pnas.0901369106

8. Tusting LS, Thwing J, Sinclair D, Fillinger U, Gimnig J, Bonner KE, et al. Mosquito larval source management for controlling malaria. Cochrane Database Syst Rev. 2013 [cited 16 Apr 2020]. doi:10.1002/14651858.CD008923.pub2

9. Carrasco-Escobar G, Manrique E, Ruiz-Cabrejos J, Saavedra M, Alava F, Bickersmith S, et al. High-accuracy detection of malaria vector larval habitats using drone-based multispectral imagery. PLoS Negl Trop Dis. 2019;13: e0007105. doi:10.1371/journal.pntd.0007105

10. Majambere S, Fillinger U, Sayer DR, Green C, Lindsay SW. Spatial Distribution of Mosquito Larvae and the Potential for Targeted Larval Control in The Gambia. Am J Trop Med Hyg. 2008;79: 19–27. doi:10.4269/ajtmh.2008.79.19

11. Grisales N, Poupardin R, Gomez S, Fonseca-Gonzalez I, Ranson H, Lenhart A. Temephos resistance in *Aedes aegypti* in Colombia compromises dengue vector control. PLoS Negl Trop Dis. 2013;7: e2438. doi:10.1371/journal.pntd.0002438

12. Organization WH. Guidelines for laboratory and field testing of mosquito larvicides. 2005 [cited 16 Apr 2020]. Available: https://apps.who.int/iris/handle/10665/69101

13. Partridge FA, Brown AE, Buckingham SD, Willis NJ, Wynne GM, Forman R, et al. An automated high-throughput system for phenotypic screening of chemical libraries on *C. elegans* and parasitic nematodes. Int J Parasitol Drugs Drug Resist. 2018;8: 8–21. doi:10.1016/j.ijpddr.2017.11.004

14. Laufer J, Roche M, Pelhate M, Elliott M, Janes NF, Sattelles DB. Pyrethroid insecticides: Actions of deltamethrin and related compounds on insect axonal sodium channels. J Insect Physiol. 1984;30: 341–349. doi:10.1016/0022-1910(84)90089-1

15. Laufer J, Pelhate M, Sattelle DB. Actions of pyrethroid insecticides on insect axonal sodium channels. Pestic Sci. 1985;16: 651–661. doi:10.1002/ps.2780160611

16. Sattelle DB, Yamamoto D. Molecular targets of pyrethroid insecticides. In: Evans PD, Wigglesworth VB, editors. Advances in Insect Physiology. Academic Press; 1988. pp. 147–213. doi:10.1016/S0065-2806(08)60025-9

17. Christophers SR. *Aëdes Aegypti* (L.), the Yellow Fever mosquito: its life history, bionomics, and structure. University Press; 1960.

18. Brackenbury J. Locomotion through use of the mouth brushes in the larva of *Culex pipiens* (Diptera: Culicidae). Proc R Soc Lond B Biol Sci. 2001;268: 101–106. doi:10.1098/rspb.2000.1336

19. Brackenbury J. Regulation of swimming in the *Culex pipiens* (Diptera, Culicidae) pupa: kinematics and locomotory trajectories. J Exp Biol. 1999;202: 2521–2529.

20. Stewart ZP, Oxborough RM, Tungu PK, Kirby MJ, Rowland MW, Irish SR. Indoor application of attractive toxic sugar bait (ATSB) in combination with mosquito nets for control of pyrethroid-resistant mosquitoes. PLOS ONE. 2013;8: e84168. doi:10.1371/journal.pone.0084168

21. Planer JD, Hulverson MA, Arif JA, Ranade RM, Don R, Buckner FS. Synergy testing of FDA-approved drugs identifies potent drug combinations against *Trypanosoma cruzi*. PLoS Negl Trop Dis. 2014;8: e2977. doi:10.1371/journal.pntd.0002977

22. Duffy S, Sykes ML, Jones AJ, Shelper TB, Simpson M, Lang R, et al. Screening the Medicines for Malaria Venture Pathogen Box across multiple pathogens reclassifies starting points for open-source drug discovery. Antimicrob Agents Chemother. 2017;61. doi:10.1128/AAC.00379-17

23. Partridge FA, Forman R, Bataille CJR, Wynne GM, Nick M, Russell AJ, et al. Anthelmintic drug discovery: target identification, screening methods and the role of open science. Beilstein J Org Chem. 2020;16: 1203–1224. doi:10.3762/bjoc.16.105

24. Partridge FA, Murphy EA, Willis NJ, Bataille CJR, Forman R, Heyer-Chauhan N, et al. Dihydrobenz[*e*][1,4]oxazepin-2(3*H*)-ones, a new anthelmintic chemotype immobilising whipworm and reducing infectivity *in vivo*. PLoS Negl Trop Dis. 2017;11: e0005359. doi:10.1371/journal.pntd.0005359

25. Partridge FA, Bataille CJR, Forman R, Marriott AE, Forde-Thomas J, Häberli C, et al. Structural Requirements for Dihydrobenzoxazepinone Anthelmintics: Actions against Medically Important and Model Parasites: *Trichuris muris*, *Brugia malayi*, *Heligmosomoides polygyrus*, and *Schistosoma mansoni*. ACS Infect Dis. 2021. doi:10.1021/acsinfecdis.1c00025

26. Partridge FA, Forman R, Willis NJ, Bataille CJR, Murphy EA, Brown AE, et al. 2,4-Diaminothieno[3,2-*d*]pyrimidines, a new class of anthelmintic with activity against adult and egg stages of whipworm. PLoS Negl Trop Dis. 2018;12: e0006487. doi:10.1371/journal.pntd.0006487

27. Sugiyama K, Katayama H, Saito T. Effect of insecticides on the mortalities of three whitefly parasitoid species, *Eretmocerusmundus*, *Eretmoceruseremicus* and *Encarsiaformosa* (Hymenoptera: Aphelinidae). Appl Entomol Zool. 2011;46: 311–317. doi:10.1007/s13355-011-0044-z

28. Ohta I, Takeda M. Acute toxicities of 42 pesticides used for green peppers to an aphid parasitoid, *Aphidius gifuensis* (Hymenoptera: Braconidae), in adult and mummy stages. Appl Entomol Zool. 2015;50: 207–212. doi:10.1007/s13355-015-0323-1

29. Jiao Y, Preston S, Song H, Jabbar A, Liu Y, Baell J, et al. Assessing the anthelmintic activity of pyrazole-5-carboxamide derivatives against *Haemonchus contortus*. Parasit Vectors. 2017;10: 272. doi:10.1186/s13071-017-2191-8

30. Kaiser HB. HI-receptor antagonist treatment of seasonal allergic rhinitis. : 4.

31. Yamashita M, Fukui H, Sugama K, Horio Y, Ito S, Mizuguchi H, et al. Expression cloning of a cDNA encoding the bovine histamine H1 receptor. Proc Natl Acad Sci. 1991;88: 11515–11519. doi:10.1073/pnas.88.24.11515

32. Hardie RC. Is histamine a neurotransmitter in insect photoreceptors? J Comp Physiol [A]. 1987;161: 201–213. doi:10.1007/bf00615241

33. Zheng Y, Hirschberg B, Yuan J, Wang AP, Hunt DC, Ludmerer SW, et al. Identification of two novel *Drosophila melanogaster* histamine-gated chloride channel subunits expressed in the eye. J Biol Chem. 2002;277: 2000–2005. doi:10.1074/jbc.M107635200

34. Roeder T. Metabotropic histamine receptors—nothing for invertebrates? Eur J Pharmacol. 2003;466: 85–90. doi:10.1016/S0014-2999(03)01553-X

35. Raymond V, Sattelle DB. Novel animal-health drug targets from ligand-gated chloride channels. Nat Rev Drug Discov. 2002;1: 427–436. doi:10.1038/nrd821

36. Bloomquist JR. Chloride channels as tools for developing selective insecticides. Arch Insect Biochem Physiol. 2003;54: 145–156. doi:10.1002/arch.10112

37. Iovchev M, Kodrov P, Wolstenholme AJ, Pak WL, Semenov EP. Altered drug resistance and recovery from paralysis in *Drosophila melanogaster* with a deficient histamine-gated chloride channel. J Neurogenet. 2002;16: 249–261. doi:10.1080/01677060216293

38. Yusein S, Velikova N, Kupenova P, Hardie R, Wolstenholme A, Semenov E. Altered ivermectin pharmacology and defective visual system in Drosophila mutants for histamine receptor HCLB. Invert Neurosci. 2008;8: 211–222. doi:10.1007/s10158-008-0078-2

39. Kita T, Irie T, Nomura K, Ozoe F, Ozoe Y. Pharmacological characterization of histamine-gated chloride channels from the housefly *Musca domestica*. NeuroToxicology. 2017;60: 245–253. doi:10.1016/j.neuro.2016.04.019

40. Pantazis A, Segaran A, Liu C-H, Nikolaev A, Rister J, Thum AS, et al. Distinct Roles for Two Histamine Receptors (hclA and hclB) at the Drosophila Photoreceptor Synapse. J Neurosci. 2008;28: 7250–7259. doi:10.1523/JNEUROSCI.1654-08.2008

41. Hemingway J. The way forward for vector control. Science. 2017;358: 998–999. doi:10.1126/science.aaj1644

42. Pirnstill CW, Coté GL. Malaria diagnosis using a mobile phone polarized microscope. Sci Rep. 2015;5: 1–13. doi:10.1038/srep13368

43. Rosado L, da Costa JMC, Elias D, Cardoso JS. Mobile-based analysis of malaria-infected thin blood smears: automated species and life cycle stage determination. Sensors. 2017;17. doi:10.3390/s17102167

44. Das DK, Mukherjee R, Chakraborty C. Computational microscopic imaging for malaria parasite detection: a systematic review. J Microsc. 2015;260: 1–19. doi:10.1111/jmi.12270

45. Moyes CL, Wiebe A, Gleave K, Trett A, Hancock PA, Padonou GG, et al. Analysis-ready datasets for insecticide resistance phenotype and genotype frequency in African malaria vectors. Sci Data. 2019;6: 121. doi:10.1038/s41597-019-0134-2

46. Hancock PA, Hendriks CJM, Tangena J-A, Gibson H, Hemingway J, Coleman M, et al. Mapping trends in insecticide resistance phenotypes in African malaria vectors. PLOS Biol. 2020;18: e3000633. doi:10.1371/journal.pbio.3000633

Figures

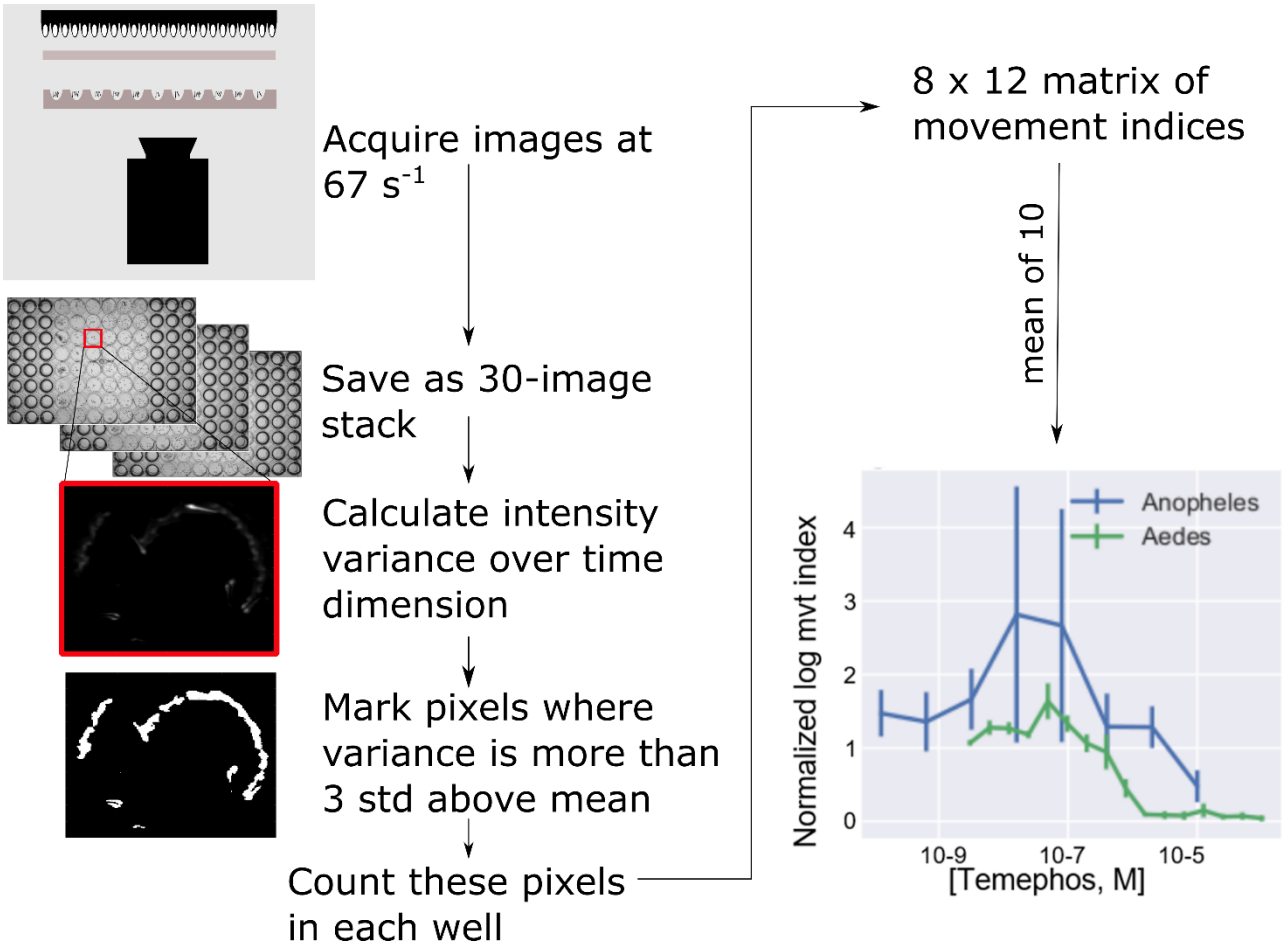

Figure 1. The procedure for automating the analysis of mosquito larval swimming. In each trial, 30 images are acquired at 10 ms intervals and stored for later offline analysis. An index of the amount of movement is obtained by measuring the variance for each pixel over time. Pixels for which the variance more than 3 standard deviations from the mean variance are scored as 1, the remainder as 0. The movement index for each well is taken as the sum of these scores for that well. The output of the algorithm for quantifying movement plotted against the concentration of temephos (bottom right), a larvicide commonly used in the control of mosquitoes, is shown at the end of the pipeline. Alongside

this similar data for larvae of *An. gambiae* are shown. A concentration-dependent inhibition of movement is seen in studies on larvae of *An. gambiae* and *Ae. aegypti*.

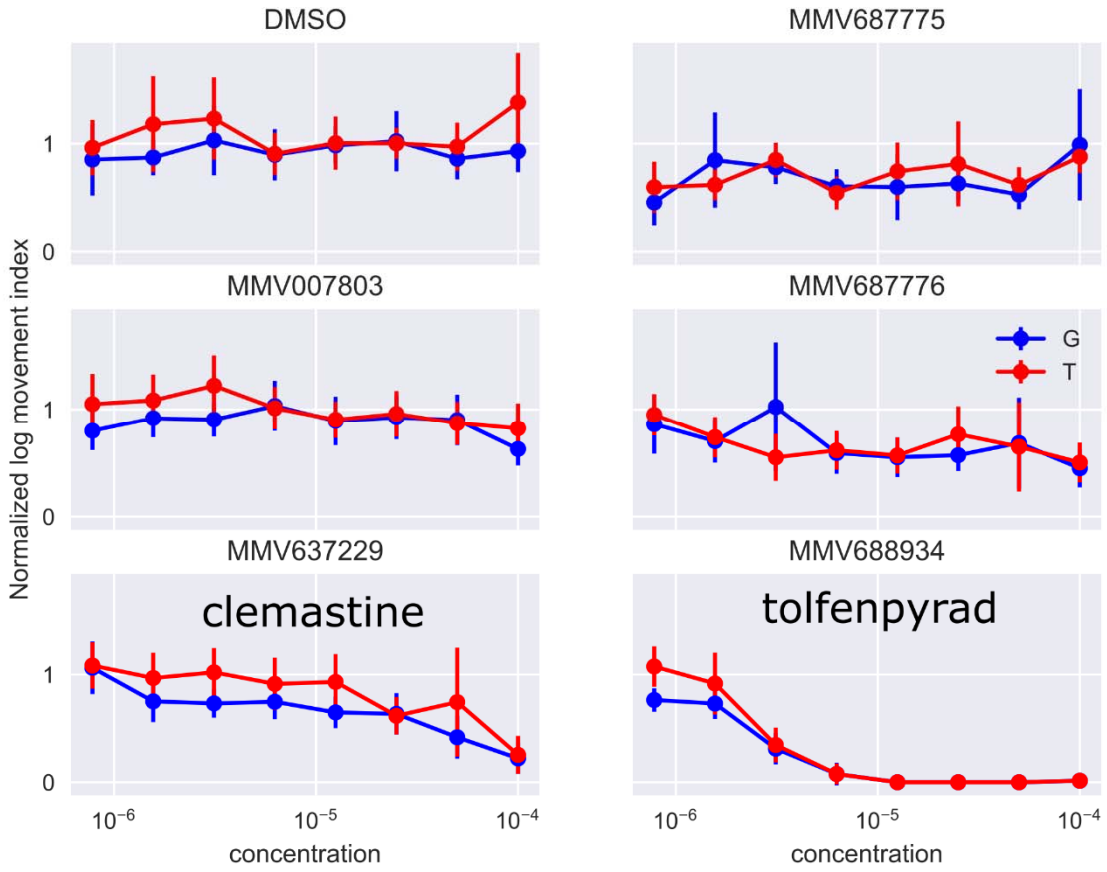

Figure 2. Screening a chemical library on *An. gambiae* larvae using the INVAPP / Paragon system. Concentration response curves for the five compounds in the Medicines for Malaria Venture (MMV) Pathogen Box library identified as active in the primary screen. The movement index for each well was measured before adding the compounds, and then again 240 min later. The second reading is divided by the first to normalize for background variations between the wells caused, for example, by differences in the number of larvae dispensed in each well. The compounds were applied over the range 3.0×10^{-9} M - 1.0×10^{-4} M, although only concentrations above 7.8×10^{-7} M are shown for

clarity. Larval progeny from both resistant *An. coluzzii* (Tiassale) and sensitive *An. gambiae* (G3) strains were studied and labelled "G" and "T" in the figure respectively. Of the compounds tested, only MMV688934 (tolfenpyrad) and MMV637229 (Clemastine) have chemical names.

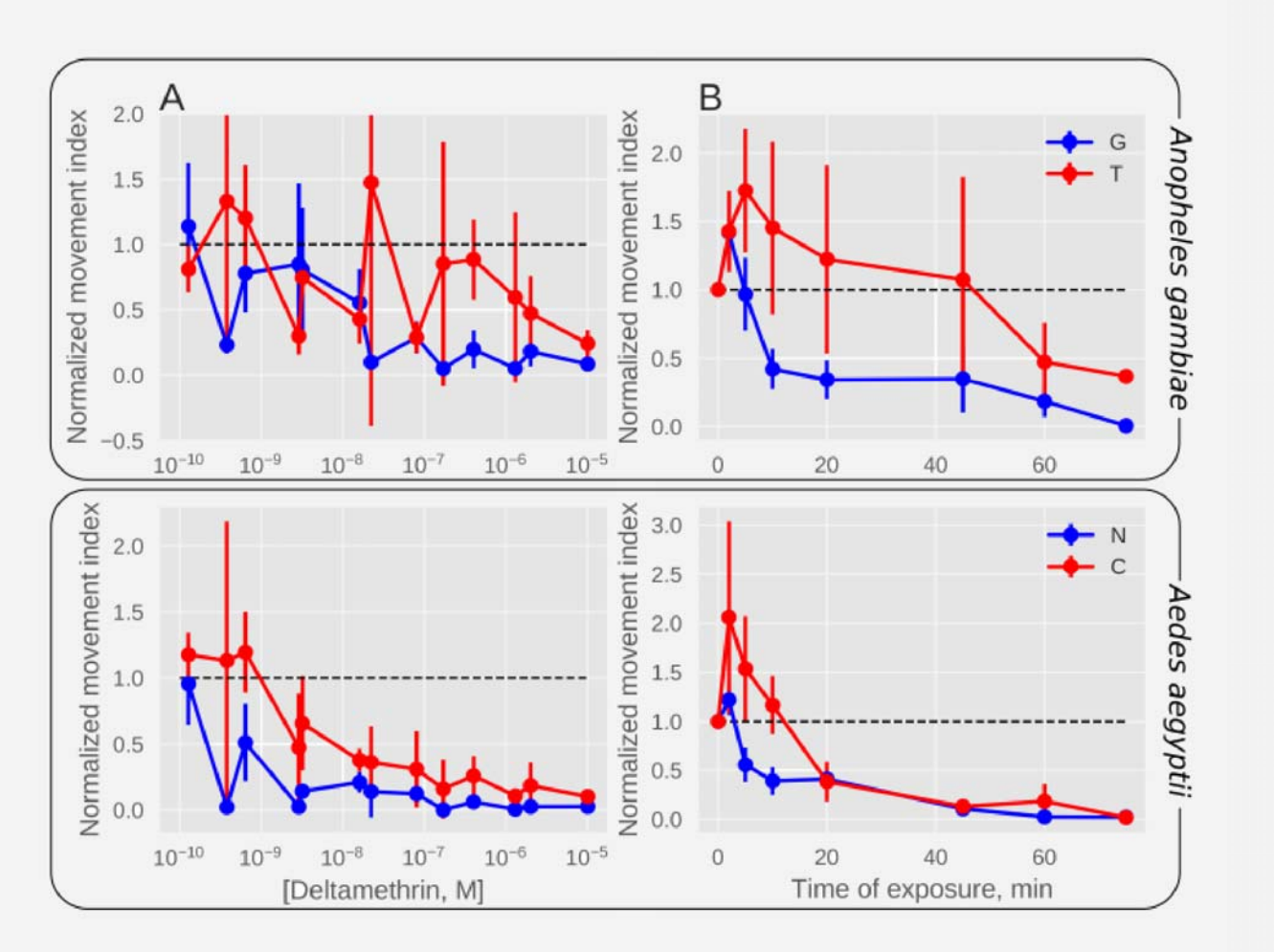

Figure 3. Motility measurement following deltamethrin exposure in concentration- and time-dependent manner for *An. Gambiae* susceptible (G3) and resistant (Tiassale) strains as well as for *Ae. Aegypti* susceptible (New Orleans) and resistant (Cayman) strains. The normalized movement index, which is the movement index (see Methods) divided by the index recorded before the application of insecticide, is plotted against the concentration after 60 min applications (A) and the time following exposure (B) to 10^{-6} M deltamethrin. Increased rate of movement inhibition is apparent in the larvae

from adult susceptible strains (blue: G3 (G), New Orleans (N)) as compared to the adult resistant strains (red: Tiassale (T), Cayman (C)). The dotted line indicates the value before insecticide application. Error bars indicate ± 1 s.e.m.

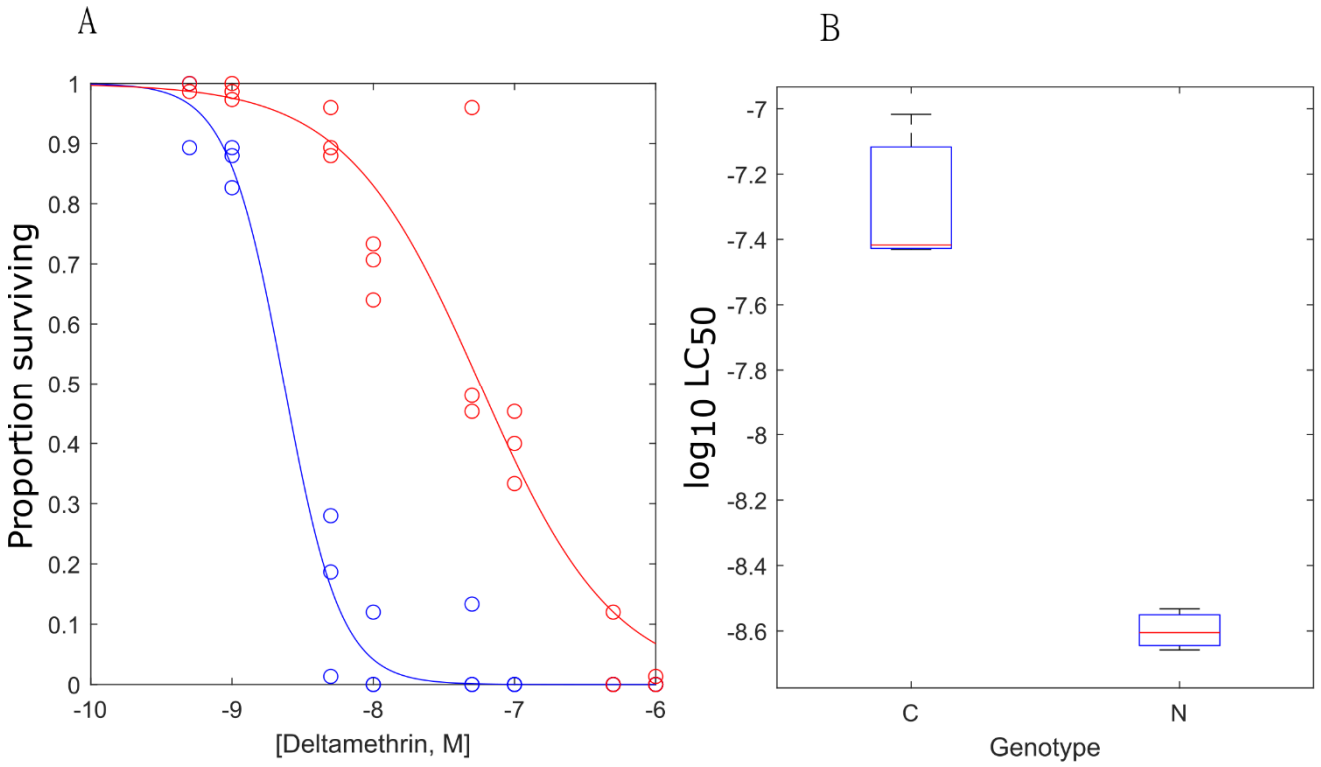

Figure 4. The application of the standard WHO larval assay to detect deltamethrin resistance in *Ae. aegypti*. Deltamethrin was tested over a range between 5.0 x 10^{-10} M to 1.0 x 10^{-6} M. (A) The concentration-response curves are given for the wild-type New Orleans strain (blue) and the Deltamethrin-resistant Cayman strain (red). (B) The fitted PIC_{50}s estimated from fitting the curves in A to a Sigmoid curve. The WHO assay yielded LC_{50}s of 8.60 ± 0.04 (2.5 nM) and 7.29 ± 0.14 (51.3 nM) for New Orleans and Cayman respectively (2-tailed, independent t-test, T(4)=-3.9, P=0.0). Each point in (B) represents the mean of 3 (WHO) separate experiments and error bars indicate the standard error of the mean.

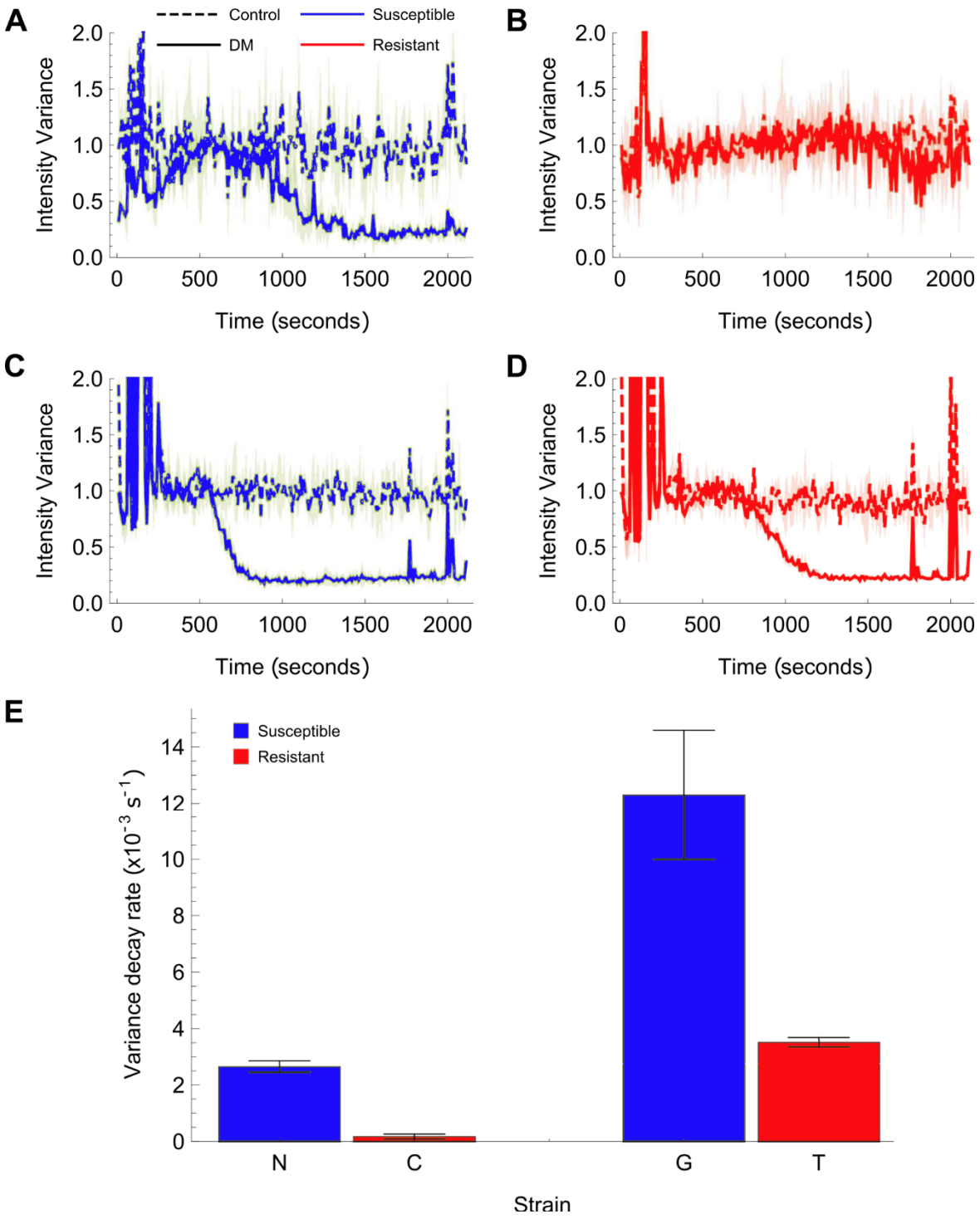

Figure 5. The output of a smartphone application that measures mosquito larvae motility following deltamethrin treatment, quantified by the average pixel variance over 2 s. (A) and (B) show the pixel

variance over time (motility) of *Aedes aegypti* New Orleans and Cayman larvae with 10^{-5} M deltamethrin in water and DMSO/water only controls. The spike at t 200s is the addition of the deltamethrin or control (water). The solid lines show the mean and the shaded area, the standard deviation (n = 3). The susceptible strain (A) motility decreases over time with DM added, whilst the resistant strain (B) does not. (C) and (D) show the pixel variance over time of *Anopheles gambiae* G3 and *An. coluzzii* Tiassale larvae with 10^{-5} M deltamethrin in water and DMSO/water controls. In this case, the resistant strain variance also decreases, but at a slower rate. (E) Fitting the variance over time of all the DM samples to exponential decay functions allows the extraction of the decay rate in each case (see methods). These are plotted on the bar chart with error bars showing the standard deviation of the fitted decay rate (n = 3). A higher decay rate is observed for the larvae from susceptible strains compared to their respective resistant strains. *Aedes aegypti* $p = 1.9 \times 10^{-5}$ (one-tailed t-test, T(2)=19.8); *Anopheles* $p = 1.1 \times 10^{-2}$ (one-tailed t-test, T(2)=6.6).

Supplementary Table S1. The top 20 hits identified in a screen of the Malaria for Medicines Venture box. The rows are sorted by the values of the movement index. The phenotype and location in the box are shown. In the "Phenotype" column, G stands for G3 (susceptible) and T for Tiassale (resistant).

Supplementary Table S2. The raw data from the Malaria for Medicines Venture box are shown, with details provided with the MMV box. In the "Phenotype" column, G stands for G3 (susceptible) and T for Tiassale (resistant).